

Designing dynamical output feedback controllers for store-operated Ca^{2+} entry

WeiJiu Liu^{a,*}, Fusheng Tang^b, Jingvoo Chen^a

^a Department of Mathematics, University of Central Arkansas, 201 Donaghey Avenue, Conway, AR 72035, USA

^b Department of Biology, University of Arkansas at Little Rock, 2801 S. University Ave., Little Rock, AR 72204-1099, USA

ARTICLE INFO

Article history:

Received 13 September 2009

Received in revised form 21 June 2010

Accepted 27 August 2010

Available online 9 September 2010

Keywords:

Store-operated calcium entry

STIM1

Orai1

Output feedback control

Stability

ABSTRACT

Store-operated calcium entry (SOCE) has been proposed as the main process controlling Ca^{2+} entry in non-excitable cells. Although recent breakthroughs in experimental studies of SOCE have been made, its mathematical modeling has not been developed. In the present work, SOCE is viewed as a feedback control system subject to an extracellular agonist disturbance and an extracellular calcium input. We then design a dynamic output feedback controller to reject the disturbance and track Ca^{2+} resting levels in the cytosol and the endoplasmic reticulum (ER). The constructed feedback control system is validated by published experimental data and its global asymptotic stability is proved by using the LaSalle's invariance principle. We then simulate the dynamic responses of STIM1 and Orai1, two major components in the operation of the store-operated channels, to the depletion of Ca^{2+} in the ER with thapsigargin, which show that: (1) Upon the depletion of Ca^{2+} in the ER, the concentrations of activated STIM1 and STIM1–Orai1 cluster are elevated gradually, indicating that STIM1 is accumulating in the ER–PM junctions and that the cytosolic portion of the active STIM1 is binding to Orai1 and driving the opening of CRAC channels for Ca^{2+} entry; (2) after the extracellular Ca^{2+} addition, the concentrations of both STIM1 and STIM1–Orai1 cluster decrease but still much higher than the original levels. We also simulate the system responses to the agonist disturbance, which show that, when a sequence of periodic agonist pulses is applied, the system returns to its equilibrium after each pulse. This indicates that the designed feedback controller can reject the disturbance and track the equilibrium.

Published by Elsevier Inc.

1. Introduction

Calcium ions play a central role in controlling dynamical cellular processes, such as insulin secretion from pancreatic beta cells [101], muscle contraction, cell proliferation, and cell death [7,80]. Intracellular calcium ions are dynamically controlled within a narrow range. Depletion of intracellular calcium stores such as the endoplasmic reticulum (ER) activates store-operated channels for Ca^{2+} entry across the plasma membrane, as demonstrated in Fig. 1. This process is called the store-operated calcium entry (SOCE), a common and ubiquitous mechanism of regulating Ca^{2+} influx into cells [1,20,80,82]. The best-studied store-operated channel (SOC) is the Ca^{2+} release-activated Ca^{2+} channel (CRAC) [12,33,34,71,82,87,107]. SOCE is necessary for the replenishment of ER Ca^{2+} content and vital for many calcium-dependent physiological processes, and it has been proposed as the main process controlling Ca^{2+} entry in non-excitable cells [81,82]. SOCE, originally known as capacitative calcium entry (CCE), was first proposed by Putney [88] and has been extensively studied later (for review, see Berridge [7,8], Bird et al [11], Chakrabarti and Chakrabarti [15], Dirksen [22], Dutta [27], Guo et al. [47], Lewis [62], Parekh

[81], Potier and Trebak [85], Prakriya and Lewis [86], Putney [90], and Shuttleworth et al. [92]).

Two major components of SOCE have been discovered: STIM1 and Orai1. STIM1 is a transmembrane protein residing primarily in the ER, but was also found on the cell surface by the immunofluorescence microscopy [74]. STIM1 contains an EF-hand, an N-terminus directed towards the lumen of the ER, and a C-terminus facing the cytoplasmic side. STIM1 functions as an endoplasmic reticulum Ca^{2+} sensor. Orai1 is a transmembrane protein present in the plasma membrane with intracellular N- and C-termini and is an essential component of the store-operated channel (for review, see Lewis [62], Potier and Trebak [85], and Putney [90]).

The mechanism about how STIM1 senses the calcium in ER and communicates with Orai1 was discovered recently (see, e.g., [21,35,41,53,62,78,82,85,90,111]). Emptying of the calcium from ER changes the conformation of STIM1 and leads to oligomerization, which enables the polybasic region to target STIM1 to ER–PM junctions, and causes a conformational change in STIM1 to expose its CRAC-activation domain (CAD, amino acids 342–448 [82]; also called SOAR (STIM1 Orai activating region), amino acids 344–442 [111]; called CCB9 (coiled-coil domain containing fragment b9), amino acids 339–446 [53]). In the junctions, the exposed STIM1 CAD binds to Orai1. STIM1–Orai1 interactions change the conformation of Orai1, which drives the opening of CRAC channels and

* Corresponding author. Tel.: +1 501 450 5684; fax: +1 501 450 5662.

E-mail address: weijiu@uca.edu (W. Liu).

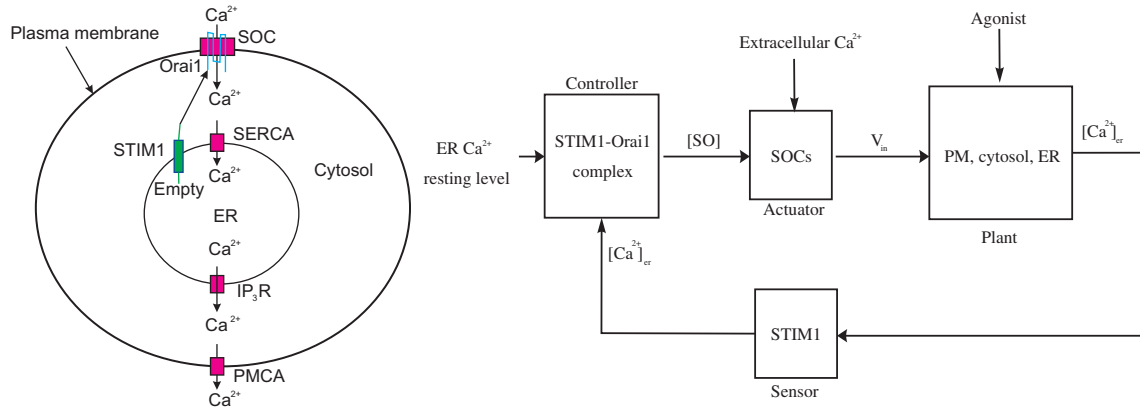


Fig. 1. A systematic sketch of an intracellular Ca^{2+} regulatory system. Left: Molecular mechanisms. Calcium ions Ca^{2+} enter the cytosol through store-operated channels (SOCs). The sarcoplasmic or endoplasmic reticulum Ca^{2+} -ATPases (SERCA) pump Ca^{2+} from the cytosol into ER and Ca^{2+} in ER are released to the cytosol through the IP_3 - and Ca^{2+} -mediated Ca^{2+} channels. Ca^{2+} exit the cytosol through the plasma membrane Ca^{2+} -ATPases (PMCA). Depletion of ER Ca^{2+} stores causes STIM1 to move to ER–PM junctions, bind to Orai1, and activate SOCs for Ca^{2+} entry. Right: A feedback control diagram.

triggers calcium entry. Moreover, the channel opening is optimized by phosphatidylinositol 4-phosphate (PI4P) (see, e.g., [60,105]) while the channel opening is disrupted by a large cell volume increase [69]. On the other hand, the CRAC channel is inactivated by calmodulin [78], annexin 6 [77], and protein kinase C [75].

To our knowledge, the mathematical modeling and analysis about SOCE have not been well developed although an elementary static feedback controller for SOCE in yeast cells was proposed recently [65,99]. Thus the aim of this paper is to fill this gap. SOCE is viewed as a feedback control system subject to an extracellular agonist disturbance and an extracellular calcium input. Based on the molecular mechanisms discovered so far (see, e.g., [21,35,41,53,62,78,82,85,90,111]), we design a dynamic output feedback controller to reject the disturbance and track Ca^{2+} resting levels in the cytosol and ER. The constructed feedback control system is validated by published experimental data of Yang et al. [108], Kim et al. [58], Liao et al. [63], and Park et al. [82], and its global asymptotic stability is proved by using the LaSalle's invariance principle. We then simulate the dynamic responses of STIM1 and Orai1 to the depletion of Ca^{2+} in the ER with thapsigargin. The simulated cytosolic Ca^{2+} dynamics and ER Ca^{2+} dynamics qualitatively agree with experimental observations of Yang et al. [108] and Yu et al. [110], showing that the cytosolic Ca^{2+} concentration increases gradually after the addition of thapsigargin and the readdition of extracellular Ca^{2+} leads to a rapid and larger increase, while the thapsigargin reduces the ER Ca^{2+} concentration from about 450 μM to about 100 μM over 5 min and the readdition of extracellular Ca^{2+} leads to a rapid increase in the ER Ca^{2+} concentration to about 10 μM . The simulation then provides a promising phenomenological prediction for the dynamics of STIM1 and Orai1: (1) Upon the depletion of Ca^{2+} in the ER, the concentrations of activated STIM1 and STIM1–Orai1 cluster are elevated gradually, indicating that STIM1 is accumulating in the ER–PM junctions and that the cytosolic portion of the active STIM1 is binding to Orai1 and driving the opening of CRAC channels for Ca^{2+} entry; (2) after the extracellular Ca^{2+} addition, the concentrations of both STIM1 and STIM1–Orai1 cluster decrease, but still much higher than their original levels. We also simulate the system responses to the agonist disturbance, showing that, when a sequence of periodic agonist pulses is applied, the system returns to its equilibrium after each pulse. This indicates that the designed feedback controller can reject the disturbance and track the equilibrium.

Since the published data on SOCE were obtained with different types of cells and SOCE is common in all types of cells, our feedback control model is constructed for generic non-excitable cells.

2. Design of dynamical output feedback controllers

As demonstrated in Fig. 1, SOCE can be viewed as a feedback control system subject to an extracellular agonist disturbance and an extracellular calcium input. The plant of the control system consists of the plasma membrane, the cytosol, and the ER with four major state variables: the cytosolic Ca^{2+} concentration $[\text{Ca}^{2+}]_c$, the buffered Ca^{2+} concentration $[\text{Ca}^{2+}]_b$, the ER Ca^{2+} concentration $[\text{Ca}^{2+}]_{er}$, and the IP_3 concentration $[\text{IP}_3]$. The sensor measuring the output $[\text{Ca}^{2+}]_{er}$ for feedback is STIM1. The actuator is the store-operated channel controlled by the STIM1–Orai1 complex concentration $[\text{SO}]$. The reference outputs to track are the cytosolic and ER Ca^{2+} resting levels.

A great number of mathematical models for the plant dynamics have been well developed by many researchers, including Albrecht et al. [2], Atri et al. [3], Bezprozvanny and Ehrlich [9], Chatton et al. [18,23–25], Keizer and De Young [55], and Sneyd et al. [94,95]. Recently Kapela et al. [52] developed a detailed mathematical model for vascular smooth muscle cells by integrating new descriptions for sub-cellular processes. Using a Monte Carlo model as a starting point, Williams et al. [106] presented an alternative formulation that solves a system of advection–reaction equations for the probability density of cytosolic and luminal domain calcium jointly distributed with IP_3 state. When these equations are coupled to ordinary differential equations for the bulk cytosolic and luminal calcium, a realistic but minimal model of whole cell Ca^{2+} dynamics is produced that accounts for the influence of local Ca^{2+} signaling on channel gating and global Ca^{2+} responses. Spatially non-homogeneous Ca^{2+} dynamics was modeled by Saftenu [91] and Hong et al. [48] using a hybrid system of reaction–diffusion equations and ordinary differential equations.

One of these models is as follows (see [95]):

$$\frac{d[\text{Ca}^{2+}]_c}{dt} = -v_{out} - v_{serca} + v_{ip} + v_{in} + k_{off}[\text{Ca}^{2+}]_b - k_{on}[\text{Ca}^{2+}]_c([\text{Ca}^{2+}]_{b,total} - [\text{Ca}^{2+}]_b), \quad (1)$$

$$\frac{d[\text{Ca}^{2+}]_{er}}{dt} = \gamma_{er}(v_{serca} - v_{ip}) + v_{stim}, \quad (2)$$

$$\frac{d[\text{Ca}^{2+}]_b}{dt} = -k_{off}[\text{Ca}^{2+}]_b + k_{on}[\text{Ca}^{2+}]_c([\text{Ca}^{2+}]_{b,total} - [\text{Ca}^{2+}]_b), \quad (3)$$

where k_{off} , k_{on} are positive constants, γ_{er} is the cytoplasmic-to-ER volume ratio, v_{out} is the Ca^{2+} efflux from the cell through the plasma

membrane calcium pump, v_{serca} is the Ca^{2+} influx into ER through the calcium pump SERCA, v_{ip} is the Ca^{2+} efflux from ER through the IP_3 -induced Ca^{2+} channel, v_{in} is the Ca^{2+} influx into the cell, and v_{stim} is the net rate of Ca^{2+} binding to and releasing from STIM1. The Eq. (3) is adopted from [48].

The Ca^{2+} entry mechanisms through SOCs have remained elusive. In yeast cells, experimental observations by Kellermayer et al. [56] and Locke et al. [70] indicated that budding yeast cells also have this store-operated calcium feedback control mechanism and the calcium uptake through SOCs follows the Michaelis–Menten equation. This Michaelis–Menten calcium uptake mechanism was used by Tang and Liu [65,99] in modeling calcium homeostasis in aging yeast cells. On the basis of these data, we assume that the SOCs follow the Michaelis–Menten kinetics and then Ca^{2+} entry into the cytosol from the extracellular environment is modeled by

$$v_{in} = V_{soc} [\text{SO}] \frac{[\text{Ca}^{2+}]_{ex}}{K_{soc} + [\text{Ca}^{2+}]_{ex}}, \quad (4)$$

where $V_{soc} > 0$ denotes the maximum rate of SOCs, K_{soc} is the Michaelis–Menten constant $[\text{Ca}^{2+}]_{ex}$ is the extracellular calcium concentration, and $[\text{SO}] = [\text{SO}]/([\text{Ca}^{2+}]_{er})$ is an output feedback controller to be designed.

The dynamic binding of the ER Ca^{2+} to STIM1 and the ER Ca^{2+} dissociation from STIM1 can be modeled by the differential equation

$$\frac{d[\text{Stim}]}{dt} = -f_s[\text{Stim}][\text{Ca}^{2+}]_{er}^{n_s} + b_s([\text{Stim}]_{total} - [\text{Stim}]), \quad (5)$$

where f_s is a binding rate, b_s is a dissociation rate, n_s is a positive exponent, and $[\text{Stim}]_{total}$ is the total concentration of STIM1. Here we assume that as soon as the ER Ca^{2+} is released from the luminal EF-hand of STIM1, the STIM1 is immediately in the ER–PM junctions. Thus $[\text{Stim}]$ can be regarded as the concentration of the active cytosolic part of STIM1 in the ER–PM junctions. The net rate of Ca^{2+} binding to and releasing from STIM1 is given by

$$v_{stim} = -f_s[\text{Stim}][\text{Ca}^{2+}]_{er}^{n_s} + b_s([\text{Stim}]_{total} - [\text{Stim}]). \quad (6)$$

The dynamic binding of the active cytosolic part of STIM1 to Orai1 and the dissociation from Orai1 can be modeled by the differential equation

$$\frac{d[\text{SO}]}{dt} = f_o(1 - [\text{SO}])[\text{Stim}] - b_o[\text{SO}], \quad (7)$$

where f_o is a binding rate, b_o is a dissociation rate, and $[\text{SO}]$ is the fraction of STIM1–Orai1 complex among the total Orai1, that is, $[\text{SO}] = \text{the concentration of STIM1–Orai1} / \text{the total concentration of Orai1}$. The term $b_o[\text{SO}] - f_o(1 - [\text{SO}])[\text{Stim}]$ is not included in the Eq. (5) because the binding of the cytosolic part of STIM1 to Orai1 does not affect the luminal part of STIM1. The Eqs. (5) and (7) constitute a dynamical output feedback controller.

To determine the values of parameters in the Eqs. (5) and (7), we read by eye the data of Fig. 1C of [71] and normalize them. Since the data were obtained at equilibrium, we find the steady state of the Eqs. (5) and (7) as follows:

$$[\text{SO}] = \frac{f_o b_s [\text{Stim}]_{total}}{b_o b_s [\text{Stim}]_{total} + b_o f_s [\text{Ca}^{2+}]_{er}^{n_s}}. \quad (8)$$

Fitting the steady state $[\text{SO}]$ into the normalized data (Fig. 2), we obtain the values of these parameters as listed in Table 1. The fitting was done by using the MATLAB curve fitting toolbox. Note that different sets of parameter values can achieve the same best fitting since the minimum difference between the data and the fitting function can attain at the different sets of values. The set of parameter values is chosen such that our model can simulate experimental data.

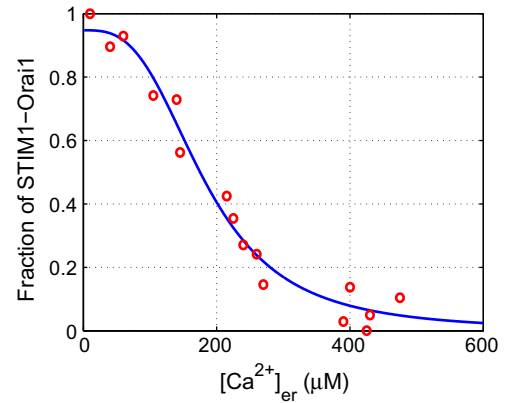


Fig. 2. Fit of the steady state $[\text{SO}]$ of the equations (5) and (7) to the normalized data (red circles) of Fig. 1C of [71], which were read by eye. (For interpretation of the references to colour in this figure legend, the reader is referred to the web version of this article.)

Table 1
Parameter values.

Parameter	Value	Reference
n_s	3	This work
f_s	$6.663 \times 10^{-6} (\text{s}^{-1} (\mu\text{M})^{-n_s})$	This work
b_s	$2.535 (\text{s}^{-1})$	This work
f_o	$1.226 (\text{s}^{-1} (\mu\text{M})^{-1})$	This work
b_o	$0.06774 (\text{s}^{-1})$	This work
$[\text{Stim}]_{total}$	$1 (\mu\text{M})$	This work
V_{soc}	Varied (see text)	This work
K_{soc}	$500 (\mu\text{M})$	[70,99]
k_{off}	$500 (\text{s}^{-1})$	[48]
k_{on}	$100 (\mu\text{M}^{-1} \text{s}^{-1})$	[48]
$[\text{Ca}^{2+}]_{b,total}$	$660 (\mu\text{M})$	[91]
v_{ip}^{ca}	$2.8 (\mu\text{M} \text{s}^{-1})$	[109]
K_m^{ca}	$1.1 (\mu\text{M})$	[55,109]
v_d^{ip}	$1 (\text{s}^{-1})$	[109]
$[\text{IP}_3]$	$0.25 (\mu\text{M})$	[109]
V_{pm}	$38 (\mu\text{M} \text{s}^{-1})$	[95]
K_{pm}	$0.5 (\mu\text{M})$	[95]
γ_{er}	5.4	[95]
v_{ip}	Varied (see text)	This work
v_{leak}	Varied (see text)	This work
V_{ser}	$100 (\mu\text{M}^{-1} \text{s}^{-1})$	This work
K_{ser}	$0.4 (\mu\text{M})$	[72,95]
I_{ser}	Varied (see text)	This work
K_{rca}	$0.077 (\mu\text{M})$	[42,73]
K_{ip3}	$3.2 (\mu\text{M})$	[42,43]
K_{inh}	$5.2 (\mu\text{M})$	[73]

Since each STIM1 has only one EF-hand, the Hill exponent n_s should be equal to 1. However, if n_s is set to 1 $[\text{SO}]$ cannot be fitted into the data. As explained by Luik et al. [71], the Hill exponent of three suggests that only oligomers of STIM1 can accumulate at ER–PM junctions.

The sarcoplasmic or endoplasmic reticulum Ca^{2+} -ATPase (SERCA), an ATP-dependent calcium pump, resides in intracellular sarcoplasmic or endoplasmic reticulum organelles and pumps Ca^{2+} from the cytosol into the organelles. We adopt Sneyd et al.'s SERCA model as follows [95]:

$$v_{serca} = \frac{V_{ser} [\text{Ca}^{2+}]_c}{(K_{ser} + [\text{Ca}^{2+}]_c) \left(1 + I_{ser} [\text{Ca}^{2+}]_{er}\right)}, \quad (9)$$

where V_{ser} , K_{ser} and I_{ser} are positive constants. The term $1 + I_{ser} [\text{Ca}^{2+}]_{er}$ describes the negative feedback of Ca^{2+} in the ER on the SERCA Ca^{2+} uptake observed by Favre et al. [31] and the parameter

I_{ser} plays a key role in determining the ER Ca^{2+} equilibrium. We add 1 to avoid the singularity when $[\text{Ca}^{2+}]_{er} = 0$.

Inositol 1,4,5-trisphosphate receptors (IP_3R), a tetramer of four identical subunits [32], function as a Ca^{2+} channel to release Ca^{2+} from the ER into the cytosol and thus play a central role in controlling the oscillations of cytosolic Ca^{2+} . A number of mathematical models for IP_3 receptors have been constructed, including Atri et al.'s model [3], Bezprozvanny et al.'s model [9], Chatton et al.'s model [18], Hagar et al.'s model [43], Keizer et al.'s model [55], Mak et al.'s model [73], Meyer et al.'s model [76], Sneyd et al.'s model [93], and Swillens et al.'s model [98]. In these models, the IP_3R was assumed to be modulated by $[\text{Ca}^{2+}]_c$ in a biphasic manner [10,37,51,83], with Ca^{2+} release inhibited by low and high $[\text{Ca}^{2+}]_c$ and facilitated by intermediate $[\text{Ca}^{2+}]_c$. Some of these models also separated the time scales of channel activation and inactivation, such that inactivation occurs on a slower time scale. In this work, we use the Mak et al.'s model.

The dependence of the IP_3R open probability on cytosolic Ca^{2+} was well fitted to a biphasic Hill equation [73]. The dependence of the IP_3R open probability on IP_3 was also well fitted to a Hill equation but with conflicting Hill exponents. According to Hagar and Ehrlich [43], the Hill exponent was found to be 1.9 in vitro. On the other hand, the Hill exponent was estimated to be about 3.5 in vivo for rat basophilic leukemia cells [76]. On the basis of these data, Fridlyand et al. [42] proposed the following IP_3R open probability model

$$P_{ip3} = \frac{[\text{Ca}^{2+}]_c}{K_{rca} + [\text{Ca}^{2+}]_c} \frac{[\text{IP}_3]^3}{K_{ip3}^3 + [\text{IP}_3]^3}.$$

Since this model did not consider the inactivation effect of cytosolic Ca^{2+} on the open probability, we add the inactivation factor $\frac{K_{inh}^3}{K_{inh}^3 + [\text{Ca}^{2+}]_c^3}$ obtained by Mak et al. [73] to obtain

$$P_{ip3} = \frac{[\text{Ca}^{2+}]_c}{K_{rca} + [\text{Ca}^{2+}]_c} \frac{K_{inh}^3}{K_{inh}^3 + [\text{Ca}^{2+}]_c^3} \frac{[\text{IP}_3]^3}{K_{ip3}^3 + [\text{IP}_3]^3}. \quad (10)$$

We tried Keizer et al.'s [55] and Sneyd et al.'s models [93]. Keizer et al.'s model worked well, but it seemed that Sneyd et al.'s model was not sensitive enough to IP_3 in simulating Ca^{2+} responses to IP_3 .

The flux of Ca^{2+} through the IP_3 -mediated channel is proportional to the number of open channels and $[\text{Ca}^{2+}]_{er} - [\text{Ca}^{2+}]_c$. Thus, the outward flux of Ca^{2+} from ER through the IP_3 mediated channel is given by

$$V_{ip} P_{ip3} ([\text{Ca}^{2+}]_{er} - [\text{Ca}^{2+}]_c),$$

where V_{ip} is the maximum flow rate. Other outward flux that we assume to be present is an outward leak, proportional to $[\text{Ca}^{2+}]_{er} - [\text{Ca}^{2+}]_c$. Thus the outward flux from the ER is

$$v_{ip} = (V_{ip} P_{ip3} + V_{leak}) ([\text{Ca}^{2+}]_{er} - [\text{Ca}^{2+}]_c), \quad (11)$$

where V_{leak} is the leak flux rate.

The equation for IP_3 production is adopted from [55,109] as follows:

$$\frac{d[\text{IP}_3]}{dt} = v_{in} p_{ip3}(t) + \frac{V_{ca}^{ip} [\text{Ca}^{2+}]_c}{K_m^{ca} + [\text{Ca}^{2+}]_c} + V_d ([\text{IP}_3] - [\text{IP}_3]), \quad (12)$$

where V_{in}^{ip} is the external IP_3 input rate, $p_{ip3}(t)$ is a pulse input caused by the extracellular agonist, V_{ca}^{ip} is the maximum Ca^{2+} dependent IP_3 input rate, V_d is the IP_3 degradation rate, K_m^{ca} is the activation constant that gives half of maximum rate of V_{ca}^{ip} , and $[\text{IP}_3]$ is the IP_3 steady state.

The model for Ca^{2+} efflux from the cytosol through the plasma membrane calcium pump is adopted from [94] as follows:

$$v_{out} = \frac{V_{pm} [\text{Ca}^{2+}]_c^2}{K_{pm}^2 + [\text{Ca}^{2+}]_c^2}, \quad (13)$$

where V_{pm} is the maximum velocity and K_{pm} is the threshold of $[\text{Ca}^{2+}]_c$ leading to half of the maximum.

3. Control model testing

The values of parameters in the feedback control system are listed in Table 1. Initial conditions are listed in Table 2. Most of parameters were adopted from the literature as indicated in Table 1. Since no data about the total STIM1 concentration are available, $[\text{Stim}]_{total}$ is taken to be $1 \mu\text{M}$. The parameters n_s , f_s , b_s , f_o , b_o are determined by fitting the steady $[\text{SO}]$ defined by (8) into the data of Luik et al. [71] (Fig. 2).

At equilibrium, we have

$$\frac{V_{pm} [\text{Ca}^{2+}]_c^2}{K_{pm}^2 + [\text{Ca}^{2+}]_c^2} = v_{out} = v_{in} = V_{soc} [\text{SO}] ([\text{Ca}^{2+}]_{ex} - [\text{Ca}^{2+}]_c)$$

and

$$\frac{V_{ser} [\text{Ca}^{2+}]_c}{(K_{ser} + [\text{Ca}^{2+}]_c)(1 + I_{ser} [\text{Ca}^{2+}]_{er})} = v_{serca} = v_{ip}.$$

Since V_{soc} and I_{ser} should be selected to result in the equilibrium calcium levels of $[\text{Ca}^{2+}]_c = 0.05 \mu\text{M}$ and $[\text{Ca}^{2+}]_{er} = 450 \mu\text{M}$ when $[\text{Ca}^{2+}]_{ex} = 1500 \mu\text{M}$, the solution of these two equations with those equilibrium calcium levels provides reference values for V_{soc} and I_{ser} . Starting from these reference values, we adjust them such that the steady states of $[\text{Ca}^{2+}]_c$ and $[\text{Ca}^{2+}]_{er}$ are close to 0.05 and $450 \mu\text{M}$, respectively.

The parameters V_{ip} , V_{leak} , and V_{ser} are adjusted in simulation such that the simulations are close to experimental observations.

The model is solved by using the function `ode15s` of MATLAB, the MathWorks, Inc. The relative error tolerance and the absolute error tolerance were set to 10^{-6} . The InitialStep is set to 0.01 and the MaxStep is set to 0.01. MATLAB does not recommend to reduce MaxStep for the accuracy of solutions since this can significantly slow down solution time. Instead the error tolerances can be used.

The resting free Ca^{2+} in the cytosol is about $0.05 \mu\text{M}$ [110] and the resting free Ca^{2+} in the ER is approximately $500 \mu\text{M}$ [40,110]. Since the model solutions during the initial transient period have no biological meanings, we solve the model with the extracellular Ca^{2+} concentration $[\text{Ca}^{2+}]_{ex}$ of $1500 \mu\text{M}$ [28] for 1500 s such that the cytosolic calcium concentration $[\text{Ca}^{2+}]_c$ achieves a steady state of about $0.05 \mu\text{M}$ (Fig. 3(middle)) and the ER calcium concentration $[\text{Ca}^{2+}]_{er}$ achieves a steady state of about $450 \mu\text{M}$ (Fig. 3(right)), and then set this moment as the initial time ($t = 0$).

Following the experiments of Yang et al. [108], before the 320th second, $[\text{Ca}^{2+}]_{ex}$ is set to $10 \mu\text{M}$, and after the 320th second $[\text{Ca}^{2+}]_{ex}$ is suddenly increased to $2000 \mu\text{M}$. After the 20th second, the maximum velocity of the Ca^{2+} pump SERCA, V_{ser} , is set to $5 \mu\text{M/s}$ to mimic the addition of thapsigargin. In this simulation, $p_{ip3}(t) \equiv 0$, $V_{ip} = 0.18 \text{ s}^{-1}$, $V_{leak} = 0.002 \text{ s}^{-1}$, $I_{ser} = 0.025 \mu\text{M}^{-1}$, and $V_{soc} = 8.85 \mu\text{M s}^{-1}$. Other parameter values are given in Table 1.

Table 2
Non-zero initial conditions.

Parameter	Value (μM)
$[\text{Ca}^{2+}]_c(0)$	0.1
$[\text{Ca}^{2+}]_{er}(0)$	150
$[\text{IP}_3](0)$	0.25

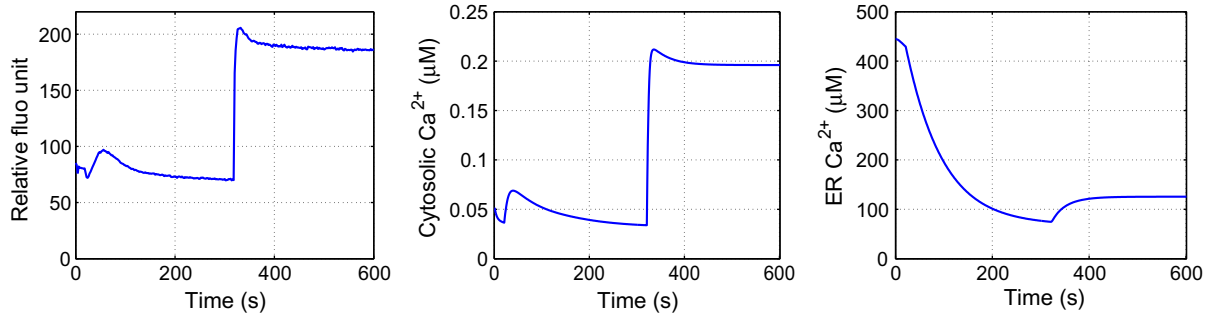


Fig. 3. SOCE simulations. Left: Reproduction of Fig. 2B of Yang et al. [108] (courtesy of S. Yang, J. Zhang, and X.-Y. Huang); middle and right: model simulations. In this simulation, $p_{IP_3}(t) \equiv 0$, $V_{IP} = 0.18 \text{ s}^{-1}$, $V_{leak} = 0.002 \text{ s}^{-1}$, $I_{ser} = 0.025 \text{ } \mu\text{M}^{-1}$, and $V_{soc} = 8.85 \text{ } \mu\text{M} \text{ s}^{-1}$. Other parameter values are given in Table 1.

The simulated cytosolic calcium dynamics plotted in Fig. 3 (middle) agrees qualitatively with the experimental data of Yang et al. [108] (Fig. 3(left)). The model simulation also agrees qualitatively with the experimental Fig. 2 Ai of Liao et al. [63] and Fig. 7E of Park et al. [82].

It was reported by Yu et al. [110] that thapsigargin reduced $[\text{Ca}^{2+}]_{er}$ from about $500 \text{ } \mu\text{M}$ to $50\text{--}100 \text{ } \mu\text{M}$ over 10 min and the readdition of extracellular Ca^{2+} led to a rapid increase in $[\text{Ca}^{2+}]_{er}$ to about $10 \text{ } \mu\text{M}$. The decrease in $[\text{Ca}^{2+}]_{er}$ was largely complete in the first minute after stimulation [110]. Fig. 3 (right) indicates that the simulated $[\text{Ca}^{2+}]_{er}$ approximately agrees with this observation.

Fig. 4 shows that as the ER Ca^{2+} decreases, the concentration of the cytosolic portion of the active STIM1 in ER-PM junctions is increasing gradually, indicating that STIM1 is accumulating in ER-PM junctions. Simultaneously, the fraction of STIM1-Orai1 is increasing gradually, indicating that the cytosolic portion of the active STIM1 is binding to Orai1 and driving the opening of CRAC channels for Ca^{2+} entry. This is consistent with the static observation of Part et al. [82]. This simulated dynamics of STIM1 and STIM1-Orai1 might provide a promising phenomenological prediction since the above argument suggests that the model could capture the main SOCE features. No data are yet available for testing this simulated dynamics.

4. Simulation of rejection of agonist disturbances

The action of an agonist on its specific receptor typically activates isoforms of the phosphoinositide-specific phospholipase C (PLC). PLC breaks down the phosphatidylinositol 4,5 bisphosphate (PIP_2) to generate two second messengers, the inositol 1,4,5 trisphosphate (IP_3) and diacylglycerol (DAG) [85]. Therefore, an agonist disturbance pulse results in an IP_3 pulse input. We assume that the pulse input is given by

$$p_{IP_3}(t) = \begin{cases} 0 & \text{if } t < 20 \text{ s,} \\ 1 & \text{if } 20 \text{ s} \leq t \leq 20.015 \text{ s,} \\ 0 & \text{if } t > 20.015 \text{ s.} \end{cases}$$

Fig. 5A shows that the pulse input of 15 ms duration causes an IP_3 pulse, and in turn, the IP_3 pulse causes Ca^{2+} release from the ER (Fig. 5B) and a transient Ca^{2+} peak in the cytosol (Fig. 5C), resulting in STIM1 accumulations in ER-PM junctions (Fig. 5D) and binding of STIM1 to Orai1 (Fig. 5E). The duration of the transient cytosolic Ca^{2+} peak is about 3 s, equal to the one observed in the experiment by Kim et al. [58] (see Fig. 2B in [58]). In this simulation, $V_{in}^{ip} = 100 \text{ } \mu\text{M} \text{ s}^{-1}$, $V_{IP} = 1.6 \text{ s}^{-1}$, $V_{leak} = 0.02 \text{ s}^{-1}$, $I_{ser} = 0.00048 \text{ } \mu\text{M}^{-1}$, and $V_{soc} = 8.85 \text{ } \mu\text{M} \text{ s}^{-1}$. Other parameter values are given in Table 1.

Furthermore, Fig. 5 shows that the ER Ca^{2+} , cytosolic Ca^{2+} , STIM1, and STIM1-Orai1 return to their resting levels, respectively, after they are disturbed by the agonist disturbance pulse. When a sequence of periodic agonist disturbance pulses is applied, Fig. 6 shows that they can also return to their resting levels after each pulse. This strongly indicates that the dynamical output feedback controller (5) and (7) can well reject the agonist disturbances. In the simulation of Fig. 6, the pulse duration is 0.05 s and $V_{in}^{ip} = 20 \text{ } \mu\text{M} \text{ s}^{-1}$. Other parameter values are the same as in Fig. 5.

5. Asymptotic stability

The global input-output stability analysis about the control system is difficult. A linear stability analysis can be always done as in [44,67], but it is not significant. Thus we focus on the global asymptotic stability.

If the extracellular calcium input $[\text{Ca}^{2+}]_{ex} = 0$, it is biologically obvious that $[\text{Ca}^{2+}]_c(t)$ and $[\text{Ca}^{2+}]_{er}(t)$ converge to 0 as $t \rightarrow \infty$. However, this stability result is not obvious mathematically and, in fact, its rigorous mathematical proof is nontrivial. We use the LaSalle's

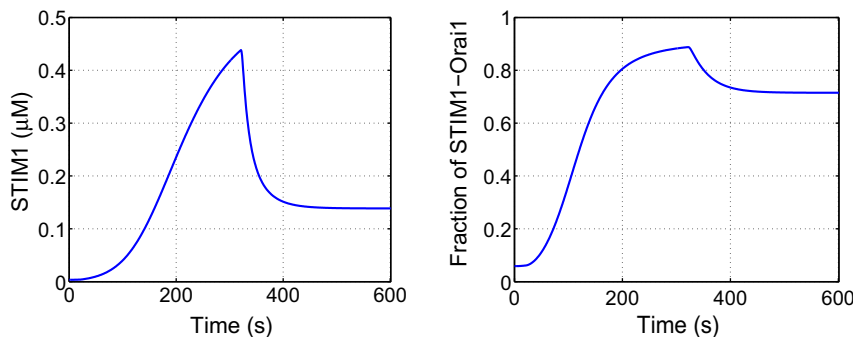


Fig. 4. Simulated dynamics of STIM1 and STIM1-bound Orai1.

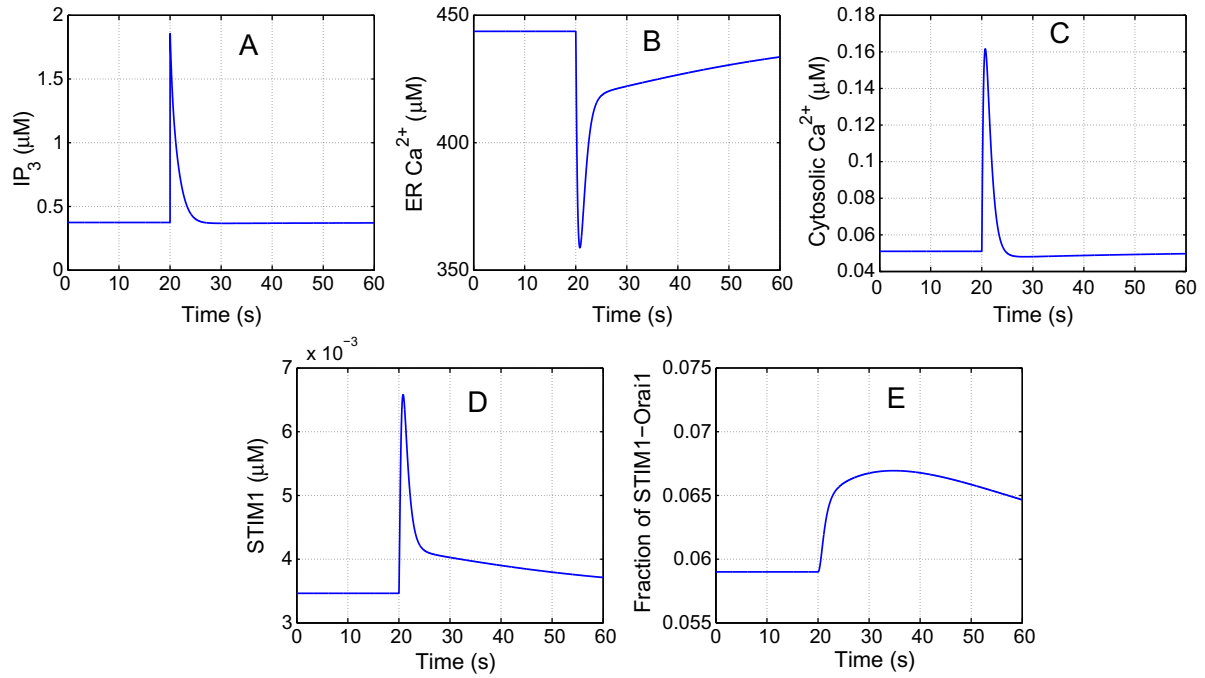


Fig. 5. Simulation of rejection of agonist disturbances. After disturbed by an agonist disturbance pulse, the ER Ca^{2+} (B), cytosolic Ca^{2+} (C), STIM1 (D), and STIM1–Orai1 (E) return to their resting levels, respectively. In this simulation, $V_{in}^{ip} = 100 \mu\text{M s}^{-1}$, $V_{ip} = 1.6 \text{ s}^{-1}$, $V_{leak} = 0.02 \text{ s}^{-1}$, $I_{ser} = 0.00048 \mu\text{M}^{-1}$, and $V_{soc} = 8.85 \mu\text{M s}^{-1}$. Other parameter values are given in Table 1.

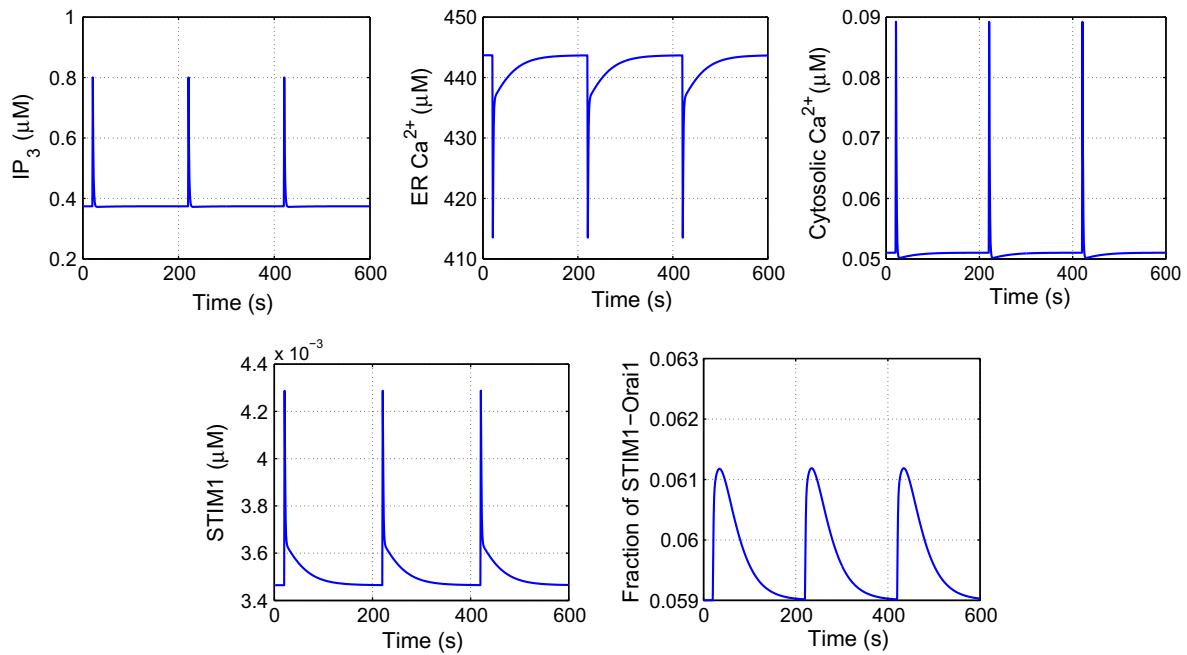


Fig. 6. Simulation of rejection of agonist disturbances. The ER Ca^{2+} , cytosolic Ca^{2+} , STIM1, and STIM1–Orai1 return to their resting levels, respectively, after each pulse of a sequence of periodic agonist disturbance pulses. In this simulation, the pulse duration is 0.0 s and $V_{in}^{ip} = 20 \mu\text{M s}^{-1}$. Other parameter values are the same as in Fig. 5.

invariance principle [57, p. 128, Theorem 4.4] to establish the asymptotic stability.

Theorem 5.1. Let $[\text{Ca}^{2+}]_{ex} = 0$ and $p_{ip3}(t) \equiv 1$. For nonnegative initial conditions with $[\text{Ca}^{2+}]_b(0) \leq [\text{Ca}^{2+}]_{b, \text{total}}$, $[\text{Stim}](0) \leq [\text{Stim}]_{\text{total}}$, and $[\text{SO}](0) \leq 1$, the solutions of the system (1), (2), (3), (5), (7), and (12) satisfy

$$\lim_{t \rightarrow \infty} [\text{Ca}^{2+}]_c(t) = \lim_{t \rightarrow \infty} [\text{Ca}^{2+}]_{er}(t) = \lim_{t \rightarrow \infty} [\text{Ca}^{2+}]_b(t) = 0, \quad (14)$$

$$\lim_{t \rightarrow \infty} [\text{IP}_3](t) = [\overline{\text{IP}_3}] + \frac{V_{in}^{ip}}{V_d^{ip}}, \quad (15)$$

$$\lim_{t \rightarrow \infty} [\text{Stim}](t) = [\text{Stim}]_{\text{total}}, \quad (16)$$

$$\lim_{t \rightarrow \infty} [\text{SO}](t) = \frac{f_o b_s [\text{Stim}]_{\text{total}}}{b_o b_s + f_o b_s [\text{Stim}]_{\text{total}}}. \quad (17)$$

In the following proof, we frequently use the result: If the real parts of all eigenvalues of a matrix M are negative and the vector function $f(t)$ converges to L as $t \rightarrow \infty$, then the solution $x(t)$ of the linear system

$$\frac{dx}{dt} = Mx + f, \quad (18)$$

converges to $-M^{-1}L$.

Let

$$\mathbb{B}_+^n = \{(x_1, x_2, \dots, x_n) \in \mathbb{R}^n | x_1, x_2, \dots, x_n \geq 0\},$$

$$\begin{aligned} \mathbb{B}_{+,Ca,K}^4 &= \{([Ca^{2+}]_c, [Ca^{2+}]_{er}, [Ca^{2+}]_b, [Stim]) \in \mathbb{R}^4 | [Ca^{2+}]_b \\ &\leq [Ca^{2+}]_{b,total}, [Stim] \leq [Stim]_{total}, \gamma_{er}([Ca^{2+}]_c + [Ca^{2+}]_b) \\ &+ [Ca^{2+}]_{er} + [Stim]_{total} - [Stim] \leq K\}, \end{aligned}$$

where $K > 0$ is selected such that $\gamma_{er}([Ca^{2+}]_c(0) + [Ca^{2+}]_b(0)) + [Ca^{2+}]_{er}(0) + [Stim](0) \leq K$. We show that $\mathbb{B}_{+,Ca,K}^4$ is positively invariant and

$$[IP_3](t), [SO](t) \geq 0 \quad (19)$$

for all $t \geq 0$. Define

$$\begin{aligned} t_0 &= \max\{T | [Ca^{2+}]_{er}(t) \geq 0 \text{ for all } 0 \leq t \leq T\}, \\ t_1 &= \max\{T | [Ca^{2+}]_c(t) \geq 0 \text{ for all } 0 \leq t \leq T\}, \\ t_2 &= \max\{T | 0 \leq [Ca^{2+}]_b(t) \leq [Ca^{2+}]_{b,total} \text{ for all } 0 \leq t \leq T\}, \\ t_3 &= \max\{T | [IP_3](t) \geq 0 \text{ for all } 0 \leq t \leq T\}, \\ t_4 &= \max\{T | 0 \leq [Stim](t) \leq [Stim]_{total} \text{ for all } 0 \leq t \leq T\}, \\ t_5 &= \max\{T | 0 \leq [SO](t) \leq 1 \text{ for all } 0 \leq t \leq T\}. \end{aligned}$$

We claim that $t_0 = t_1 = t_2 = t_3 = t_4 = t_5 = \infty$. If it was not true, then $t^* = \min\{t_0, t_1, t_2, t_3, t_4, t_5\} < \infty$. We may as well assume that $t_0 = t^*$. Then $[Ca^{2+}]_{er}(t) < 0$, $[Ca^{2+}]_c(t) \geq 0$, $0 \leq [Ca^{2+}]_b(t) \leq [Ca^{2+}]_{b,total}$, $0 \leq [Stim](t) \leq [Stim]_{total}$, and $0 \leq [SO](t) \leq 1$ for all $0 \leq t \leq t_0$ and $[Ca^{2+}]_{er}(t_0) = 0$. It then follows from (2), (9), and (11) that

$$\begin{aligned} \frac{d[Ca^{2+}]_{er}}{dt} \Big|_{t_0} &= \gamma_{er} \frac{V_{ser}[Ca^{2+}]_c(t_0)}{(K_{ser} + [Ca^{2+}]_c(t_0))} + \gamma_{er}(V_{ip}P_{ip3} + V_{leak})[Ca^{2+}]_c(t_0) \\ &+ b_s([Stim]_{total} - [Stim](t_0)) \geq 0. \end{aligned}$$

If either $[Ca^{2+}]_c(t_0) > 0$ or $0 \leq [Stim](t_0) < [Stim]_{total}$, then $\frac{d[Ca^{2+}]_{er}}{dt} \Big|_{t_0} > 0$. Thus $[Ca^{2+}]_{er}(t)$ is increasing near t_0 and then $[Ca^{2+}]_{er}(t) < [Ca^{2+}]_{er}(t_0) = 0$ for some $t < t_0$. This is a contradiction. Hence $[Ca^{2+}]_c(t_0) = 0$ and $[Stim](t_0) = [Stim]_{total}$. Then it follows from (1) that

$$\frac{d[Ca^{2+}]_c}{dt} \Big|_{t_0} = k_{off}[Ca^{2+}]_b(t_0).$$

If $[Ca^{2+}]_b(t_0) > 0$, then $\frac{d[Ca^{2+}]_c}{dt} \Big|_{t_0} > 0$. Thus $[Ca^{2+}]_c(t)$ is increasing near t_0 and then $[Ca^{2+}]_c(t) < [Ca^{2+}]_c(t_0) = 0$ for some $t < t_0$. This is a contradiction and so $[Ca^{2+}]_b(t_0) = 0$. It then follows from (1), (2), (3), (5), (7), and (12) that $[Ca^{2+}]_c(t) = [Ca^{2+}]_{er}(t) = [Ca^{2+}]_b(t) = 0$, $[Stim](t) = [Stim]_{total}$, $[IP_3](t) \geq 0$, and $0 \leq [SO](t) \leq 1$ for $t \geq t_0$. This contradicts with $t^* = \min\{t_0, t_1, t_2, t_3, t_4, t_5\} < \infty$. Define

$$V = \gamma_{er}([Ca^{2+}]_c + [Ca^{2+}]_b) + [Ca^{2+}]_{er} + [Stim]_{total} - [Stim].$$

It follows from (1), (2), (3), and (5) that

$$\frac{dV}{dt} = -\frac{\gamma_{er}V_{pm}[Ca^{2+}]_c^2}{K_{pm}^2 + [Ca^{2+}]_c^2} - \gamma_{er}V_{soc}[SO][Ca^{2+}]_c \leq 0.$$

Thus $\mathbb{B}_{+,Ca,K}^4$ is positively invariant. Because

$$\begin{aligned} Z &= \left\{ \left([Ca^{2+}]_c, [Ca^{2+}]_{er}, [Ca^{2+}]_b, [Stim] \right) \in \mathbb{B}_{+,Ca,K}^4 \mid \frac{dV}{dt} = 0 \right\} \\ &= \left\{ \left(0, [Ca^{2+}]_{er}, [Ca^{2+}]_b, [Stim] \right) \in \mathbb{B}_{+,Ca,K}^4 \right\}, \end{aligned}$$

it follows from the LaSalle's invariance principle [57, p.128, Theorem 4.4] that

$$\lim_{t \rightarrow \infty} [Ca^{2+}]_c(t) = 0.$$

For $\alpha > 1$, we can deduce from the Eqs. (2) and (5) that

$$\begin{aligned} \frac{d}{dt} ([Ca^{2+}]_{er} + \alpha([Stim]_{total} - [Stim])) \\ = -F(t, \alpha)([Ca^{2+}]_{er} + \alpha([Stim]_{total} - [Stim])) + f(t), \end{aligned}$$

where $\lim_{t \rightarrow \infty} f(t) = 0$ and $F(t, \alpha) \geq F_0 > 0$ for all $t \geq 0$ if α is sufficiently close to 1. It therefore follows that:

$$\lim_{t \rightarrow \infty} ([Ca^{2+}]_{er}(t) + \alpha([Stim]_{total} - [Stim](t))) = 0.$$

In the same way, we deduce that

$$\lim_{t \rightarrow \infty} [Ca^{2+}]_b(t) = 0.$$

From the Eq. (12), we deduce that

$$\lim_{t \rightarrow \infty} [IP_3](t) = [\overline{IP_3}] + \frac{V_{ip}^{ip}}{V_{in}^{ip}}.$$

6. Discussion

In this modeling, we assumed that as soon as the ER Ca^{2+} is released from the luminal EF-hand of STIM1, the STIM1 is immediately in the ER-PM junctions. This assumption may be refined by introducing two state variables: $[Stim]_{er}$ for the ER luminal portion of STIM1 and $[Stim]_c$ for the cytosolic portion. These two states may be connected by the equation

$$\frac{d[Stim]_c}{dt} = k([Stim]_{er} - [Stim]_c),$$

where the positive constant k is a rate of conformational change from $[Stim]_{er}$ to $[Stim]_c$.

Since the binding of STIM1 to both C and N termini is required to activate the CRAC channel [82], the feedback controller (5)–(7) may be refined by introducing three binding states: $[SO]_N$ for the state of STIM1 binding to the N terminus of Orai1, $[SO]_C$ for the state of STIM1 binding to the C terminus of Orai1, and $[SO]_{CN}$ for the state of STIM1 binding to both C and N termini of Orai1. The difficulty in this modeling is how to model the change of one state to another. In addition, since clustering and activation of CRAC channels are separable processes [82], the controller may be improved by introducing two states: $[SO]_{clu}$ for the clustering and $[SO]_a$ for the activation. Again the problem is how to model the switch between these two states.

Stochastic factors were neglected in our modeling. Like telephone calls arriving at a switchboard, agonists arrive at the plasma membrane randomly and independently. Thus the agonist action on the plasma membrane, $p_{ip3}(t)$, should follow a Poisson process. In addition, the extracellular calcium $[Ca^{2+}]_{ex}$ may be fluctuated randomly and then contain random 'noises'. These stochastic factors should be taken into account to further refine the model.

The distributions of Ca^{2+} in the cytosol and ER are not uniform and the Ca^{2+} concentrations near the ER are higher. The modeling of these spatial Ca^{2+} distributions leads to the PDE model [54]:

$$\begin{aligned}
\frac{\partial [\text{Ca}^{2+}]_c}{\partial t} &= \nabla \cdot (D_c \nabla [\text{Ca}^{2+}]_c) - v_{\text{buf}} \quad \text{in } \Omega_c, \\
\frac{\partial [\text{Ca}^{2+}]_{er}}{\partial t} &= \nabla \cdot (D_{er} \nabla [\text{Ca}^{2+}]_{er}) + v_{\text{stim}} \quad \text{in } \Omega_{er}, \\
\frac{d[\text{Ca}^{2+}]_b}{dt} &= v_{\text{buf}} \quad \text{in } \Omega_c, \\
\frac{\partial [IP_3]}{\partial t} &= \nabla \cdot (D_{ip3} \nabla [IP_3]) + v_{ca}^{ip} - v_d^{ip} [IP_3] \quad \text{in } \Omega_c, \\
D_c \nabla [\text{Ca}^{2+}]_c \cdot \mathbf{n} &= v_{in} - v_{out} \quad \text{on } \partial_{pm} \Omega_c, \\
D_c \nabla [\text{Ca}^{2+}]_c \cdot \mathbf{n} &= -D_{er} \nabla [\text{Ca}^{2+}]_{er} \cdot \mathbf{n} = v_{ip} - v_{serca} \quad \text{on } \partial \Omega_{er}, \\
D_{ip3} \nabla [IP_3] \cdot \mathbf{n} &= V_{in}^{ip} p_{ip3}(t) \quad \text{on } \partial_{pm} \Omega_c, \\
\nabla [IP_3] \cdot \mathbf{n} &= 0 \quad \text{on } \partial \Omega_{er},
\end{aligned}$$

where D 's denote the diffusivity, Ω_c denotes the cytoplasm domain, Ω_{er} denotes the ER domain, $\partial_{pm} \Omega_c$ denotes the cell plasma membrane, $\partial \Omega_{er}$ denotes the boundary of the ER, \mathbf{n} is the unit outward normal vector of a domain, and

$$v_{\text{buf}} = -k_{\text{off}}[\text{Ca}^{2+}]_b + k_{\text{on}}[\text{Ca}^{2+}]_c ([\text{Ca}^{2+}]_{b,\text{total}} - [\text{Ca}^{2+}]_b).$$

This leads to the problem of designing the boundary controller v_{in} .

The ER part of STIM1 can be still modeled by (5) with a modification:

$$\begin{aligned}
\frac{d[\text{Stim}]_{er}}{dt} &= -f_s[\text{Stim}]_{er} \left(\frac{1}{\text{mes}(\Omega_{er})} \int_{\Omega_{er}} [\text{Ca}^{2+}]_{er} dV \right)^{n_s} \\
&\quad + b_s([\text{Stim}]_{\text{total}} - [\text{Stim}]_{er}).
\end{aligned}$$

The movement of the cytosolic part of STIM1 from the ER region to the ER–PM junction can be modeled by the transport equation:

$$\begin{aligned}
\frac{\partial [\text{Stim}]_c}{\partial t} &= \mathbf{v} \cdot \nabla [\text{Stim}]_c \quad \text{in } \Omega_c, \quad [\text{Stim}]_c = [\text{Stim}]_{er} \quad \text{on } \partial \Omega_{er}, \\
[\text{Stim}]_c &= 0 \quad \text{on } \partial_{pm} \Omega_c,
\end{aligned}$$

where \mathbf{v} is a velocity field. Since Orai1 is in the plasma membrane and is not diffusive, the ODE model (7) can be kept with a little change:

$$\frac{d[\text{SO}]}{dt} = \frac{f_o}{\text{mes}(\Omega_{er-pm})} (1 - [\text{SO}]) \int_{\Omega_{er-pm}} [\text{Stim}]_c dV - b_o[\text{SO}],$$

where Ω_{er-pm} is the ER–PM junction domain. It is evident that these PDE control models are too complicated to validate and make any progress, so simplifying assumptions will be needed. To this end, the homogenization technique [5,54,68] may be needed.

Controllability and observability are important structure properties of a dynamical system. These control properties for the system (1), (2), (3), (5), (7), and (12) may be analyzed as done in [44].

Calcium ions play a central role in the process of insulin secretion. Release of calcium ions from intracellular stores is essential for the amplification of insulin secretion by promoting the replenishment of the readily releasable pool of secretory granules, while voltage-dependent calcium entry is directed to the sites of exocytosis via the binding of the L-type calcium channels to SNARE proteins [100,101]. Therefore, the SOCE model will have potential applications in modeling insulin secretion [66,67].

Acknowledgments

We thank Dr. X.-Y. Huang for providing the data on SOCE [108] to validate our model (Fig. 3) and Dr. S. Yang for pointing recent publications by Richard Lewis' group and Tobias Meyer's group, such as [12,82], to us. We thank two reviewers for spending their precious time on evaluating this manuscript and giving constructive comments, which greatly improved this manuscript. Liu was supported by the University Research Council Fund of the University of Central Arkansas. Research in Tang's laboratory was supported by the Kathleen Thomsen Hall Charitable Trust Fund and the American Heart Association (09BGIA290189).

References

- [1] Iskandar F. Abdullaev, Jonathan M. Bisailon, Marie Potier, Jose C. Gonzalez, Rajender K. Motiani, Mohamed Trebak, Stim1 and Orai1 Mediate CRAC currents and store-operated calcium entry important for endothelial cell proliferation, *Circ. Res.* 103 (2008) 1289.
- [2] Meredith A. Albrecht, Stephen L. Colegrove, David D. Friel, Differential regulation of ER Ca^{2+} uptake and release rates accounts for multiple modes of Ca^{2+} -induced Ca^{2+} release, *J. Gen. Physiol.* 119 (2002) 211.
- [3] Alireza Atri, Jeff Amundson, David Clapham, James Sneyd, A single-pool model for intracellular calcium oscillations and waves in the *Xenopus laevis* oocyte, *Biophys. J.* 65 (1993) 1727.
- [5] A. Bensoussan, J.-L. Lions, G. Papanicolaou, *Asymptotic Analysis for Periodic Structures*, North-Holland Pub. Co., New York, 1978.
- [7] Michael J. Berridge, Elementary and global aspects of calcium signalling, *J. Physiol.* 499 (1997) 291.
- [8] M.J. Berridge, M.D. Bootman, H.L. Roderick, Calcium signalling: dynamics, homeostasis and remodelling, *Nat. Rev. Mol. Cell. Biol.* 4 (2003) 517.
- [9] Ilya Bezprozvanny, Barbara E. Ehrlich, Inositol (1,4,5)-trisphosphate (InsP_3)-gated Ca channels from cerebellum: conduction properties for divalent cations and regulation by intraluminal calcium, *J. Gen. Physiol.* 104 (1994) 821.
- [10] Ilya Bezprozvanny, James Watras, Barbara E. Ehrlich, Bell-shaped calcium-response curve of $\text{Ins}(1,4,5)\text{P}_3$ - and calcium-gated channels from endoplasmic reticulum of cerebellum, *Nature* 351 (1991) 751.
- [11] Gary S. Bird, Wayne I. DeHaven, Jeremy T. Smyth, James W. Putney Jr., Methods for studying store-operated calcium entry, *Methods* 46 (2008) 204.
- [12] Onn Brandman, Jen Liou, Wei Sun Park, Tobias Meyer, STIM2 is a feedback regulator that stabilizes basal cytosolic and endoplasmic reticulum Ca^{2+} levels, *Cell* 131 (2007) 1327.
- [15] Ranjana Chakrabarti, Rabindranath Chakrabarti, Calcium signaling in non-excitable cells: Ca^{2+} release and influx are independent events linked to two plasma membrane Ca^{2+} entry channels, *J. Cell. Biochem.* 99 (2006) 1503.
- [18] Jean-Yves Chatton, Yumei Cao, Jörg W. Stucki, Perturbation of myo-inositol-1,4,5-trisphosphate levels during agonist-induced Ca^{2+} oscillations, *Biophys. J.* 74 (1998) 523.
- [20] Wayne DeHaven, Bertina Jones, John Petranka, Jeremy Smyth, Takuro Tomita, Gary Bird James Putney, TRPC channels function independently of STIM1 and Orai1, *J. Physiol.* 587 (2009) 2275.
- [21] Isabella Derler, Marc Fahrner, Oliviero Carugo, Martin Muik, Judith Bergsmann, Rainer Schindl, Irene Frischauf, Said Eshaghi, Christoph Romanin, Increased hydrophobicity at the N-terminus/membrane interface impairs gating of the SCID-related ORAI1 mutant, *J. Biol. Chem.* 284 (2009) 15903.
- [22] Robert T. Dirksen, Checking your SOCCs and feet: the molecular mechanisms of Ca^{2+} entry in skeletal muscle, *J. Physiol.* 587 (2009) 3139.
- [23] G. Dupont, A. Goldbeter, One-pool model for Ca^{2+} oscillations involving Ca^{2+} and inositol 1,4,5-trisphosphate as co-agonists for Ca^{2+} release, *Cell Calcium* 14 (1993) 311.
- [24] Genevieve Dupont, Albert Goldbeter, Properties of intracellular Ca^{2+} waves generated by a model based on Ca^{2+} -induced Ca^{2+} release, *Biophys. J.* 67 (1994) 2191.
- [25] Genevieve Dupont, Stephane Swillens, Quantal release, incremental detection, and long-period Ca^{2+} oscillations in a model based on regulatory Ca^{2+} -binding sites along the permeation pathway, *Biophys. J.* 71 (1996) 1714.
- [27] D. Dutta, Mechanism of store-operated calcium entry, *J. Biosci.* 25 (2000) 397.
- [28] Melita M. Dvorak, Ashia Siddiqua, Donald T. Ward, D. Howard Carter, Sarah L. Dallas, Edward F. Nemeth, Daniela Riccardi, Physiological changes in extracellular calcium concentration directly control osteoblast function in the absence of calciotropic hormones, *Proc. Natl. Acad. Sci. USA* 101 (2004) 5140.
- [31] Cecile J. Favre, Jacques Schrenzel, Jean Jacquet, Daniel P. Lew, Karl-Heinz Krause, Highly supralinear feedback inhibition of Ca^{2+} uptake by the Ca^{2+} load of intracellular stores, *J. Biol. Chem.* 271 (1996) 14925.
- [32] C.D. Ferris, R.L. Haganir, S. Supattapone, S.H. Snyder, Purified inositol 1,4,5-trisphosphate receptor mediated calcium flux in reconstituted lipid vesicles, *Nature* 342 (1989) 87.
- [33] Stefan Feske, Murali Prakriya, Anjana Rao, Richard S. Lewis, A severe defect in CRAC Ca^{2+} channel activation and altered K^+ channel gating in T cells from immunodeficient patients, *J. Exp. Med.* 202 (2005) 651.
- [34] Stefan Feske, Yousang Gwack, Murali Prakriya, Sonal Srikanth, Sven-Holger Puppel, Bogdan Tanasa, Patrick G. Hogan, Richard S. Lewis, Mark Daly, Anjana Rao, A mutation in Orai1 causes immune deficiency by abrogating CRAC channel function, *Nature* 441 (2006) 179.
- [35] Stefan Feske, ORAI1 and STIM1 deficiency in human and mice: roles of store-operated Ca^{2+} entry in the immune system and beyond, *Immunol. Rev.* 231 (2009) 189.
- [37] E.A. Finch, T.J. Turner, S.M. Goldin, Calcium as a coagonist of inositol 1,4,5-trisphosphate-induced calcium release, *Science* 252 (1991) 443.
- [40] Irene Frischauf, Rainer Schindl, Isabella Derler, Judith Bergsmann, Marc Fahrner, Christoph Romanin, The STIM/Orai coupling machinery, *Channels* 2 (2008) 1.

- [41] Irene Frischauf, Martin Muik, Isabella Derler, Judith Bergsmann, Marc Fahrner, Rainer Schindl, Klaus Groschner, Christoph Romanin, Molecular determinants of the coupling between STIM1 and Orai channels, differential activation of Orai1C3 channels by a Stim1 coiled-coil mutant, *J. Biol. Chem.* 284 (2009) 21696.
- [42] Leonid E. Fridlyand, Natalia Tamarina, Louis H. Philipson, Modeling of Ca^{2+} flux in pancreatic β -cells: role of the plasma membrane and intracellular stores, *Am. J. Physiol. Endocrinol. Metab.* 285 (2003) E138.
- [43] R.E. Hagar, B.E. Ehrlich, Regulation of the type III $\text{InsP}(3)$ receptor by $\text{InsP}(3)$ and ATP, *Biophys. J.* 79 (2000) 271.
- [44] Ramesh Garimella, Uma Garimella, Weijiu Liu, A theoretic control approach in a signal-controlled metabolic pathway, *Math. Biosci. Eng.* 4 (2007) 471.
- [47] Rui-wei Guo, Lan Huang, New insights into the activation mechanism of store-operated calcium channels: roles of STIM and Orai, *J. Zhejiang Univ. Sci. B* 9 (2008) 591.
- [48] Dihui Hong, Dov Jaron, Donald G. Buerk, Kenneth A. Barbee, Transport-dependent calcium signaling in spatially segregated cellular caveolar domains, *Am. J. Physiol. Cell Physiol.* 294 (2008) C856.
- [51] Suresh K. Joseph, Howard L. Rice, John R. Williamson, The effect of external calcium and pH on inositol trisphosphate-mediated calcium release from cerebellar microsomal fractions, *Biochem. J.* 258 (1989) 261.
- [52] Adam Kapela, Anastasios Bezerianos, Nikolaos M. Tsoukias, A mathematical model of Ca^{2+} dynamics in rat mesenteric smooth muscle cell: agonist and NO stimulation, *J. Theor. Biol.* 253 (2008) 238.
- [53] Takumi Kawasaki, Ingo Lange, Stefan Feske, A minimal regulatory domain in the C terminus of STIM1 binds to and activates ORAI1 CRAC channels, *Biochem. Biophys. Res. Commun.* 385 (2009) 49.
- [54] J. Keener, J. Sneyd, *Mathematical Physiology*, vols. 1 and 2., second ed., Springer, New York, 2009.
- [55] Joel Keizer, Gary W. De Young, Two roles for Ca^{2+} in agonist stimulated Ca^{2+} oscillations, *Biophys. J.* 61 (1992) 649.
- [56] Richard Kellermayer, David P. Aiello, Attila Miseta, David M. Bedwell, Extracellular Ca^{2+} sensing contributes to excess Ca^{2+} accumulation and vacuolar fragmentation in a $\text{pmr1}\Delta$ mutant of *S. cerevisiae*, *J. Cell Sci.* 116 (2003) 1637.
- [57] H.K. Khalil, *Nonlinear Systems*, Prentice Hall, New Jersey, 2002.
- [58] Sang Jeong Kim, Yunju Jin, Jun Kim, Jung Hoon Shin, Paul F. Worley, David J. Linden, Transient upregulation of postsynaptic IP_3 -gated Ca release underlies short-term potentiation of mGluR1 signaling in cerebellar purkinje Cells, *J. Neurosci.* 28 (2008) 4350.
- [60] Marek K. Korzenowski, Marko A. Popovic, Zsolt Szentpetery, Peter Varnai, Stanko S. Stojilkovic, Tamas Balla, Dependence of STIM1/Orai1-mediated calcium entry on plasma membrane phosphoinositides, *J. Biol. Chem.* 284 (2009) 21027.
- [62] Richard S. Lewis, The molecular choreography of a store-operated calcium channel, *Nature* 446 (2007) 284.
- [63] Yanhong Liao, Christian Exleben, Eda Yildirim, Joel Abramowitz, David L. Armstrong, Lutz Birnbaumer, Orai proteins interact with TRPC channels and confer responsiveness to store depletion, *Proc. Natl. Acad. Sci. USA* 401 (2007) 4682.
- [65] W. Liu, F. Tang, An output feedback controller for store-operated calcium entry and extracellular calcium sensing in yeast cells, in: *Proceedings of the 22nd Chinese Control and Decision Conference*, May 26–28, 2010, Xuzhou, China, 2010, pp. 3748–3753.
- [66] W. Liu, C. Hsin, F. Tang, A molecular mathematical model of glucose mobilization and uptake, *Math. Biosci.* 221 (2009) 121.
- [67] Weijiu Liu, Fusheng Tang, Modeling a simplified regulatory system of blood glucose at molecular levels, *J. Theor. Biol.* 252 (2008) 608.
- [68] W. Liu, Does a fast mixer really exist?, *Phys. Rev. E* 72 (2005) 016312.
- [69] Xibao Liu, Hwei Ling Ong, Biswaranjan Pani, Katherine Johnson, William B. Swaim, Brij Singh, Indu Ambudkar, Effect of cell swelling on ER/PM junctional interactions and channel assembly involved in SOCE, *Cell Calcium* 47 (2010) 491.
- [70] E.G. Locke, M. Bonilla, L. Liang, Y. Takita, K.W. Cunningham, A homolog of voltage-gated Ca^{2+} channels stimulated by depletion of secretory Ca^{2+} in yeast, *Mol. Cell. Biol.* 20 (2000) 6686.
- [71] Riina M. Luik, Bin Wang, Murali Prakriya, Minnie M. Wu, Richard S. Lewis, Oligomerization of STIM1 couples ER calcium depletion to CRAC channel activation, *Nature* 454 (2008) 538.
- [72] Jonathan Lytton, Marisa Westlin, Scott E. Burk, Gary E. Shull, David H. MacLennan, Functional comparisons between isoforms of the sarcoplasmic or endoplasmic reticulum family of calcium pumps, *J. Biol. Chem.* 267 (1992) 14483.
- [73] D.O. Mak, S. McBride, J.K. Foskett, Regulation by Ca^{2+} and inositol 1,4,5-trisphosphate (InsP_3) of single recombinant type 3 InsP_3 receptor channels. Ca^{2+} activation uniquely distinguishes types 1 and 3 insp_3 receptors, *J. Gen. Physiol.* 117 (2001) 435.
- [74] S.S. Manji, N.J. Parker, R.T. Williams, L. van Stekelenburg, R.B. Pearson, M. Dziadek, P.J. Smith, STIM1: a novel phosphoprotein located at the cell surface, *Biochim. Biophys. Acta* 1481 (2000) 147.
- [75] Stuart P. McElroy, Robert M. Drummond, Alison M. Gurney, Regulation of store-operated Ca^{2+} entry in pulmonary artery smooth muscle cells, *Cell Calcium* 46 (2009) 99.
- [76] T. Meyer, T. Wensel, L. Stryer, Kinetics of calcium channel opening by inositol 1,4,5-trisphosphate, *Biochemistry* 29 (1990) 32.
- [77] Katia Monastyrskaya, Eduard B. Babychuk, Andrea Hostettler, Peta Wood, Thomas Grewal, Annette Draeger, Plasma membrane-associated annexin A6 reduces Ca^{2+} entry by stabilizing the cortical actin cytoskeleton, *J. Biol. Chem.* 284 (2009) 17227.
- [78] F.M. Mullins, C.Y. Park, R.E. Dolmetsch, R.S. Lewis, STIM1 and calmodulin interact with Orai1 to induced Ca^{2+} -dependent interaction of CRAC channels, *Proc. Natl. Acad. Sci. USA* 106 (2009) 15495.
- [80] A.B. Parekh, J.W. Putney Jr., Store-operated calcium channels, *Physiol. Rev.* 85 (2005) 757.
- [81] Anant B. Parekh, On the activation mechanism of store-operated calcium channels, *Pflugers Arch. Eur. J. Physiol.* 453 (2006) 303.
- [82] Chan Young Park, Paul J. Hoover, Franklin M. Mullins, Priti Bachhawat, Elizabeth D. Covington, Stefan Raunser, Thomas Walz, K. Christopher Garcia, Ricardo E. Dolmetsch, Richard S. Lewis, STIM1 clusters and activates CRAC channels via direct binding of a cytosolic domain to Orai1, *Cell* 136 (2009) 876.
- [83] I. Parker, I. Ivorra, Inhibition by Ca^{2+} of inositol trisphosphate-mediated Ca^{2+} liberation: a possible mechanism for oscillatory release of Ca^{2+} , *Proc. Natl. Acad. Sci. USA* 87 (1990) 260.
- [85] Marie Potier, Mohamed Trebak, New developments in the signaling mechanisms of the store-operated calcium entry pathway, *Pflugers Arch.* 457 (2008) 405.
- [86] Murali Prakriya, Richard S. Lewis, CRAC channels: activation, permeation, and the search for a molecular identity, *Cell Calcium* 33 (2003) 311.
- [87] Murali Prakriya, Richard S. Lewis, Regulation of CRAC channel activity by recruitment of silent channels to a high open-probability gating mode, *J. Gen. Physiol.* 128 (2006) 373.
- [88] J.W. Putney Jr., A model for receptor-regulated calcium entry, *Cell Calcium* 7 (1986) 1.
- [90] J.W. Putney Jr., Recent breakthroughs in the molecular mechanism of capacitative calcium entry (with thoughts on how we got here), *Cell Calcium* 42 (2007) 103.
- [91] E.E. Saftenu, Computational study of non-homogeneous distribution of Ca^{2+} handling systems in cerebellar granule cells, *J. Theor. Biol.* 257 (2009) 228.
- [92] Trevor J. Shuttlesworth, Jill L. Thompson, Olivier Mignen, STIM1 and the noncapacitative ARC channels, *Cell Calcium* 42 (2007) 183.
- [93] James Sneyd, Jean-François Dufour, A dynamic model of the type-2 inositol trisphosphate receptor, *Proc. Natl. Acad. Sci. USA* 99 (2002) 2398.
- [94] J. Sneyd, K. Tsaneva-Atanasova, J.I.E. Bruce, S.V. Straub, D.R. Giovannucci, D.I. Yule, A model of calcium waves in pancreatic and parotid acinar cells, *Biophys. J.* 85 (2003) 1392.
- [95] J. Sneyd, K. Tsaneva-Atanasova, D.I. Yule, J.L. Thompson, T.J. Shuttlesworth, Control of calcium oscillations by membrane fluxes, *Proc. Natl. Acad. Sci. USA* 101 (2004) 1392.
- [98] S. Swillens, L. Combettes, P. Champeil, Transient inositol 1,4,5-trisphosphate-induced Ca^{2+} release: a model based on regulatory Ca^{2+} -binding sites along the permeation pathway, *Proc. Natl. Acad. Sci. USA (Biophys.)* 91 (1994) 10074.
- [99] F. Tang, W. Liu, An age-dependent feedback control model for calcium in yeast cells, *J. Math. Biol.* 60 (6) (2010) 849.
- [100] Natalia A. Tamarina, Andrey Kuznetsov, Louis H. Philipson, Reversible translocation of YFP-tagged STIM1 is coupled to calcium influx in insulin secreting β -cells, *Cell Calcium* 44 (2008) 533.
- [101] Anders Tengholm, Erik Gylfe, Oscillatory control of insulin secretion, *Mol. Cell. Endocrinol.* 297 (2009) 58.
- [105] Ciara M. Walsh, Michael Chvanov, Lee P. Haynes, Ole H. Petersen, Alexei V. Tepikin, Robert D. Burgoyne, Role of phosphoinositides in STIM1 dynamics and store-operated calcium entry, *Biochem. J.* 425 (2010) 159.
- [106] George S.B. Williams, Evan J. Molinelli, Gregory D. Smith, Modeling local and global intracellular calcium responses mediated by diffusely distributed inositol 1,4,5-trisphosphate receptors, *J. Theor. Biol.* 253 (2008) 170.
- [107] Minnie M. Wu, JoAnn Buchanan, Riina M. Luik, Richard S. Lewis, Ca^{2+} store depletion causes STIM1 to accumulate in ER regions closely associated with the plasma membrane, *J. Cell Biol.* 174 (2006) 803.
- [108] Shengyu Yang, J. Jillian Zhang, Xin-Yun Huang, Orai1 and STIM1 are critical for breast tumor cell migration and metastasis, *Cancer Cell* 15 (2009) 124.
- [109] G.W. De Young, J. Keizer, A single-pool inositol 1,4,5-trisphosphate-receptor-based model for agonist-stimulated oscillations in Ca^{2+} concentration, *Proc. Natl. Acad. Sci. USA* 89 (1992) 9895.
- [110] Run Yu, Patricia M. Hinkle, Rapid turnover of calcium in the endoplasmic reticulum during signaling, *J. Biol. Chem.* 275 (2000) 23648.
- [111] Joseph P. Yuan, Weizhong Zeng, Michael R. Dorwart, Young-Jin Choi, Paul F. Worley, Shmuel Muallem, SOAR and the polybasic STIM1 domains gate and regulate Orai channels, *Nat. Cell Biol.* 11 (2009) 337.